ON THE USE OF PLANAR SCATTERING PROBLEM TECHNIQUES TO ANALYZE THIN PLANAR QUASI-MAGNETO-STATIC SHIELDING

by

Charles D. Hechtman,† Erik H. Lenzing,‡ and Barry S. Perlman ‡

ABSTRACT

A metallic screen scattering technique developed for microwave and millimeter wave applications is adapted, using the principle of duality to a quasi-magnetostatic shielding problem. In the limiting case of low frequency (0.01 Hz) the results compare favorably with the static solution. Moreover, this adaptation is expanded to treat finite permeability shields.

1. INTRODUCTION

In the past there has been numerous examples of borrowing and adapting methods and techniques across disciplines, for example Harrington's adaptation of the method of moments[1] for electromagnetics or the use of electrostatics for specialized wire-routing problems.[2] In this work a scattering technique, usually applied to conductive screens at high frequency and the principle of duality, is applied to quasi-static and static magnetic field shielding problems.

Magnetic fields emanating from static and quasi-static sources such as power lines or permanent magnets are often considered undesirable and require mitigation. Attenuation may be provided locally by shields designed for quasi-static and static fields. These shield designs rely upon material properties, e.g., high permeability, and geometric configuration, e.g., thin inhomogeneous sheeting, to satisfy engineering and economic requirements. The large number of possible shield designs warrants simulation and modeling to optimize shield efficacy and provide manufacturing cost control.

Traditionally, shield geometries are analyzed at zero frequency with an assortment of techniques that solve Laplace's equation. Analytic solutions, which provide the most insight, are most tractable in 2 dimensions, where conformal mapping is available. Moreover, geometries found in most magnetostatic problems do not have analytic solutions. Therefore, most static field solutions are found numerically in terms of a scalar potential using techniques such as a finite difference[3] or finite element method[3] or in terms of a boundary charge distribution using techniques such as a static moment method[3] or a static spectral domain method.[3]

For the limiting case of thin shields with finite permeability in free space, the methods identified above are problematic. Using the finite difference or finite element techniques would require an enormous numbers of grids or elements in and around the regions of the shield. Such conditions spawn an inefficient, huge set of equations and other problems are associated with their solutions. In addition, the static moment method or the static spectral domain method are only effective for infinite permeability. In contrast, the quasi-magneto-static problem could be posed as a scattering problem for both infinite and finite permeability where the resulting magnetic field integral equation (MFIE) is solved with a moment method[4] in the spatial domain (most effective for non-periodic structures) or in the spectral domain[5] (effective for periodic and non-periodic structures). Both of these methods would be useful for planar shields and could be modified for truncated cylindrical shields.

In the next sections the shielding problem is recast into a quasi-static scattering problem with infinite permeability. The results are compared with the static solution and the result is generalized to finite permeability.

† Stevens Institute of Technology, Castle Point on the Hudson, Hoboken, New Jersey 07030

‡ U.S. Army Research Lab, EPSD, Microwave and Photonics Division, Ft. Monmouth, New Jersey

2. *A scattering problem with infinite permeability*

Scattering problems commonly have feature sizes on the order of a wavelength. In this example we consider feature sizes (several meters) that are a small fraction of the wavelength (λ approximately 3,000 miles). This is still a scattering problem, given the proviso of non-zero frequency, where phase retardation exists between the shield and source. An illustrative example appears in figure 1 for the 2 dimensional version. The left hand side consists of a typical scattering problem, where an electric field is incident on a perfectly conducting strip. An electric surface current is induced on the strip with a resulting scattered electric field that nulls the incident electric field on the surface.

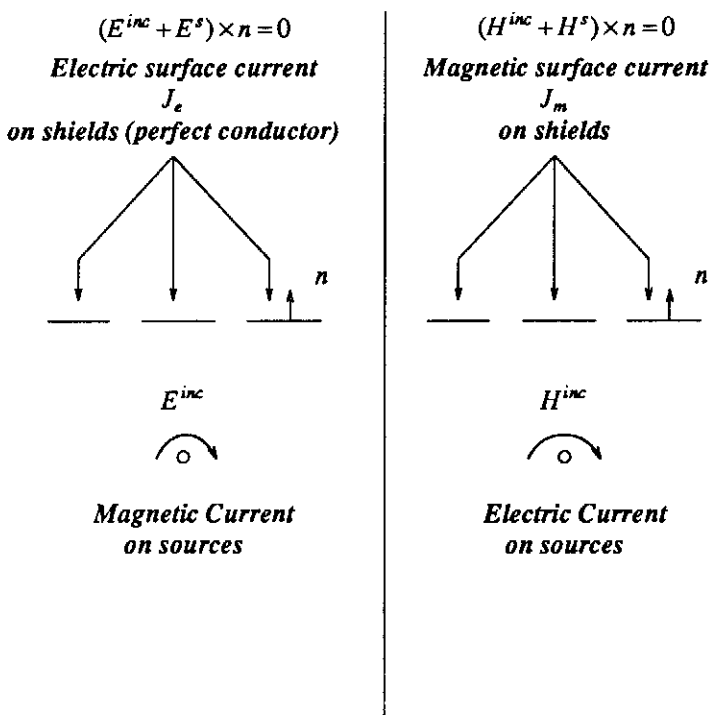

Figure 1. Two dimensional scattering, Electric and Magnetic Duality

On the right hand side similar field behavior exists for the magnetic field. The electric and magnetic field scattering problems are equivalent and are related by the principle of duality.[6] In what follows the formulation is developed in terms of the electric field.

Initially, for the case of infinite conductivity (infinite permeability) the sum of the tangential incident electric field, E^{inc}, and the scattered electric field, E^{scat}, must be zero.

$$(E^{inc}+E^{scat})\times n=0\,. \tag{1}$$

The electric field integral equation (EFIE) corresponding to the special case of two dimension strips on the $y = 0$ plane (geometry and coordinates shown in Figure 2) and an incident electric field that contains only an x component is given by

$$E_x^{inc}+\int_{strip} J_{ex}(x')g(x,x')dx'=0\,, \tag{2}$$

where x is a coordinate on the shields,

$$g(x)=-\frac{\beta\eta}{8}[H_0^{(2)}(|\beta x|)+H_2^{(2)}(|\beta x|)]\,, \tag{3}$$

is a 2-D modified Green's function that describes the scattered electric field on the strip, $H_i^{(2)}$ is a Hankel function of second kind, and β is the wave number. This EFIE may be found in Balanis[7] with a detailed dervation presented in the Appendix of this paper. Determining the correct current density on the strips, $J_e(x)$, for the integral equation (2) is the key task in this problem. This may be accomplished in a number

of ways with various levels of approximation. The scattered electric field may then be determined for all space by,

$$E^{scat}(r) = \int_{strip} J_{ex}(r')g(r,r')dr', \tag{4}$$

where r is a position vector and $E^{inc}(r)$ is the incident electric field.

2.1 Point Collocation Method[8]

The point collocation method is a familiar technique[8] that satisfies the boundary condition (1) at discrete points only. Boundary segments off these points may not be satisfied. Hence, the resulting current density distribution and the scattered field are only an approximation. The current expansion is in terms of pulse functions.

The following test case will demonstrate the efficacy of this technique. While applying the point collocation method, the Green's function was approximated as follows:

$$g(x) = -\frac{\beta\eta}{8}[H_0^{(2)}(|\beta x|) + H_2^{(2)}(|\beta x|)] \approx -\frac{\beta\eta}{8}[1 + \frac{(\beta x)^2}{8} - j(\frac{2}{\pi}\ln(\frac{\gamma|\beta x|}{2}) - \frac{4}{\pi x^2})] \ , \tag{5}$$

where η is the free space impedance and $\ln(\gamma = 1.781)$ is Euler's constant. Referring to figure 2, two infinitesimally thin shields lie on the abscissa, each of length $L=1$ separated by a distance $W=0$ (i.e., a single shield of length 2 centered about the origin).

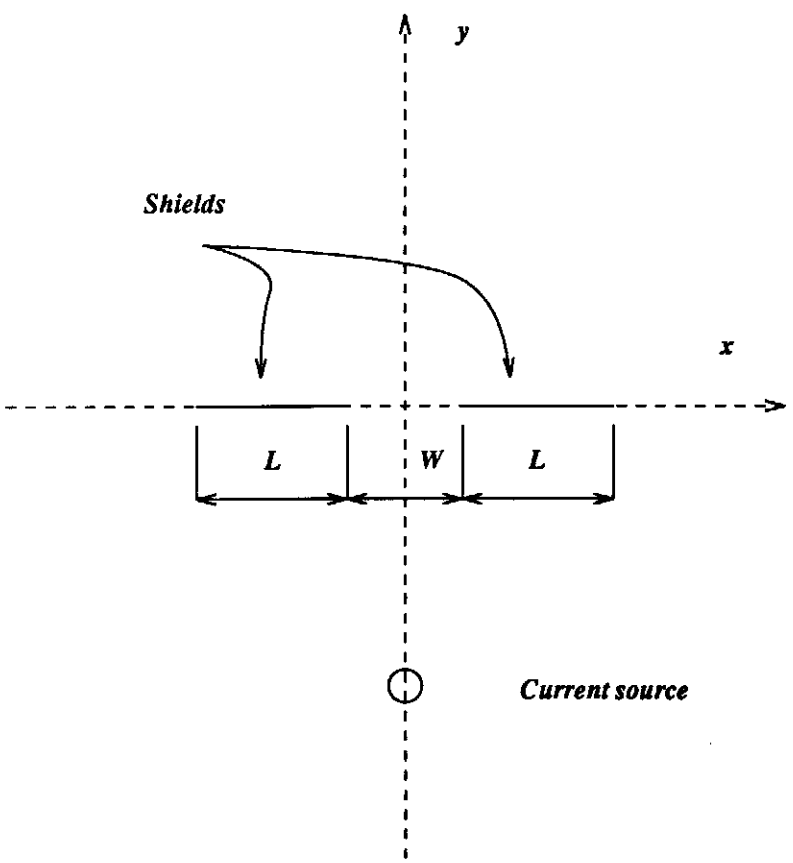

Figure 2. Test case shield geometry

The shields are of infinite permeability and an electric current source is located -5 meters beneath the origin. An analytic solution found by conformal mapping exists for this geometry and is compared with the collocation point matching solution, in figure 3.

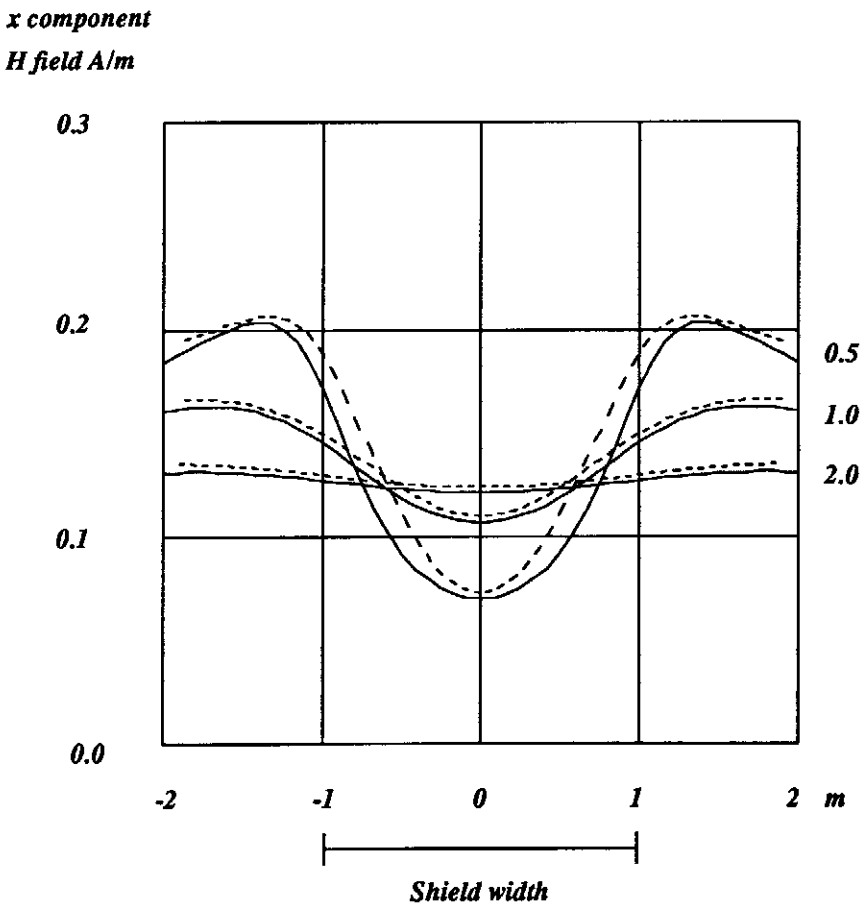

Figure 3. Comparison of H_x variation with x when $y = 0.5, 1.0, 2.0$, where dashed lines represent conformal mapping solution and the solid lines represent the point collocation method

The x component of the magnetic field for the analytic solution (dashed lines) and the point matching solution (solid lines) using 20 points are plotted as a function of x for $y = 0.5, 1.0, 2.0$. The case where $y = 0.5$ shows the largest error, $\leq 15\%$, and as y increases the deviation decreases. This is expected since the 20 discrete boundary points appear to smear with larger distance. Increasing the number of points improves the result marginally but the spectral domain method outlined in the next section is a better choice. Figures 4,5, and 6 are three dimensional plots of the variation of the x component of the electric field for shields separated by $W = 0.5, 0.1, 0.0$ meters and length, $L = 1$ meters, centered at the origin. Figures 4 and 5 show the magnetic field leaking through the shield gap. These pictures clearly illustrate the shielding futility in using long strips perpendicular to the magnetic field lines.

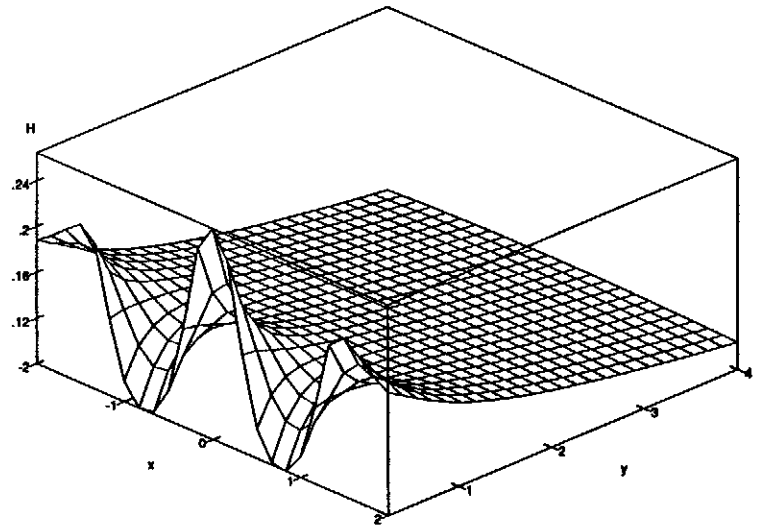

FIGURE 4. MAGNETIC FIELD VARIATION WITH POSITION FOR THE CASE OF TWO SHIELDS 1 METER WIDE SEPARATED BY 0.5 METERS WITH A SOURCE AT -5 METERS

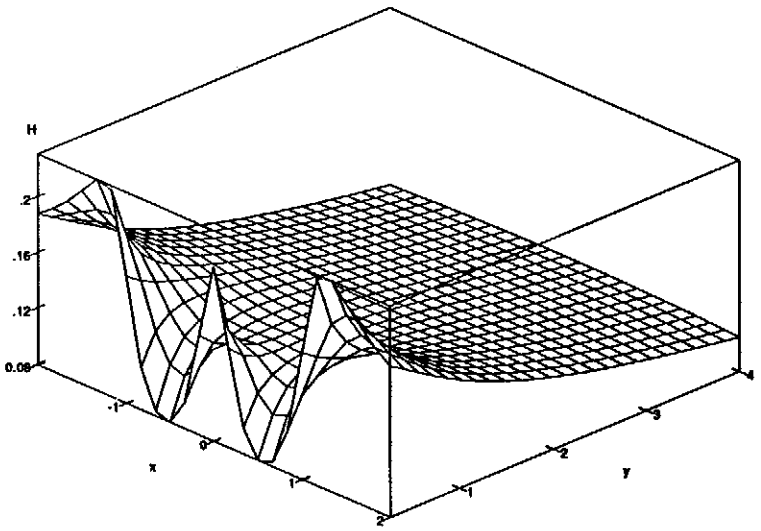

FIGURE 5. MAGNETIC FIELD VARIATION WITH POSITION FOR THE CASE OF TWO SHIELDS 1 METER WIDE SEPARATED BY 0.1 METERS WITH A SOURCE AT -5 METERS

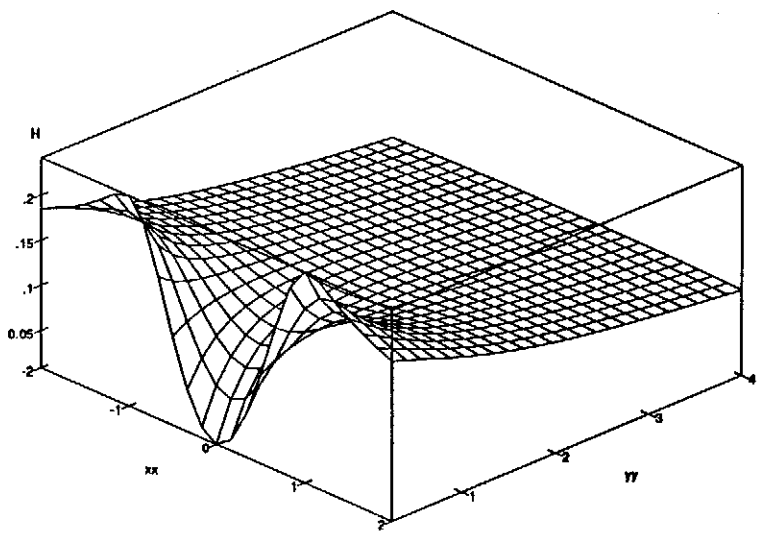

FIGURE 6. MAGNETIC FIELD VARIATION WITH POSITION FOR THE CASE OF TWO SHIELDS 1 METER WIDE SEPARATED BY 0.0 METERS WITH A SOURCE AT -5 METERS

2.2 Spectral Domain Method[5] and finite permeability

Whereas the point collocation method seeks to satisfy the boundary condition at discrete points on the boundary, the Spectral Domain Method seeks to force uniform convergence of the boundary condition in the fourier transform domain. The Fourier transform of the EFIE yields

$$\tilde{E}^{inc}(\alpha)+\tilde{J}_e(\alpha)\tilde{g}(\alpha)=\tilde{E}^{total}(\alpha) \tag{6}$$

where the tilde represents the fourier transform of the function and the Fourier transform pair is defined as

$$\tilde{E}(\alpha)=\int_{-\infty}^{\infty}E(x)e^{-j\alpha x}dx \tag{7}$$

and

$$E(x)=\frac{1}{2\pi}\int_{-\infty}^{\infty}\tilde{E}(\alpha)e^{j\alpha x}d\alpha\ . \tag{8}$$

The Fourier transform of the Green's function (equation (3)) is given by

$$\tilde{g}(\alpha)=-\int_{-\infty}^{\infty}\frac{\beta\eta}{8}[H_0^{(2)}(|\beta x|)+H_2^{(2)}(|\beta x|)]\ e^{-j\alpha x}dx=-\frac{\eta}{\beta}\sqrt{\beta^2-\alpha^2}\ . \tag{9}$$

See Appendix A of C. Scott[5] for derivation. The current may be represented as a sum of aperture-limited basis functions with unknown coefficients and appropriate edge condition,[1] where for the strip above

$$\tilde{J}_e(\alpha)=\sum_{n=1}^{N}a_n\tilde{\psi}_n(\alpha) \tag{10}$$

and

$$\psi_n(x)=a_n\frac{\cos(nx\pi/2)}{\sqrt{x^2-1}}\ . \tag{11}$$

Multiplication and integration of equation (6) with $\tilde{\psi}_n(\alpha)$ yields the following:

$$\int_{-\infty}^{\infty}\tilde{\psi}_n(\alpha)\tilde{E}^{inc}(\alpha)d\alpha+\int_{-\infty}^{\infty}\tilde{\psi}_n(\alpha)\sum_{m=1}^{N}a_m\tilde{\psi}_M(\alpha)(-\frac{\eta}{\beta}\sqrt{\beta^2-\alpha^2})d\alpha= \tag{12}$$

$$\int_{-\infty}^{\infty}\tilde{\psi}_n(\alpha)\tilde{E}^{total}(\alpha)d\alpha\quad n=1,2,...,N\ ,$$

where for the case of infinite conductivity (or infinite permeability) $\tilde{E}^{total}(\alpha)=0$. Therefore there are N equations in N unknowns where the values of a_m are the constants to be determined. This determines the current on the shield where N is chosen for the desired degree of accuracy. Of course, the choice of basis functions is critical for rapid convergence.

The following plot (figure 7) revisits the two dimensional example of the last section where the magnetic field is computed above a shield 2 meters wide with a line source -5 meters beneath the thin high permeability shield. This plot illustrates the use of one well chosen basis function, namely N=1, from equation (12) for the determination of the field 0.5 meters above the shield and is compared with the corresponding conformal mapping solution.

1. Aperture with infinitely sharp edges require that the current density vector follow specific behavior near the edge. This is known as the edge condition.

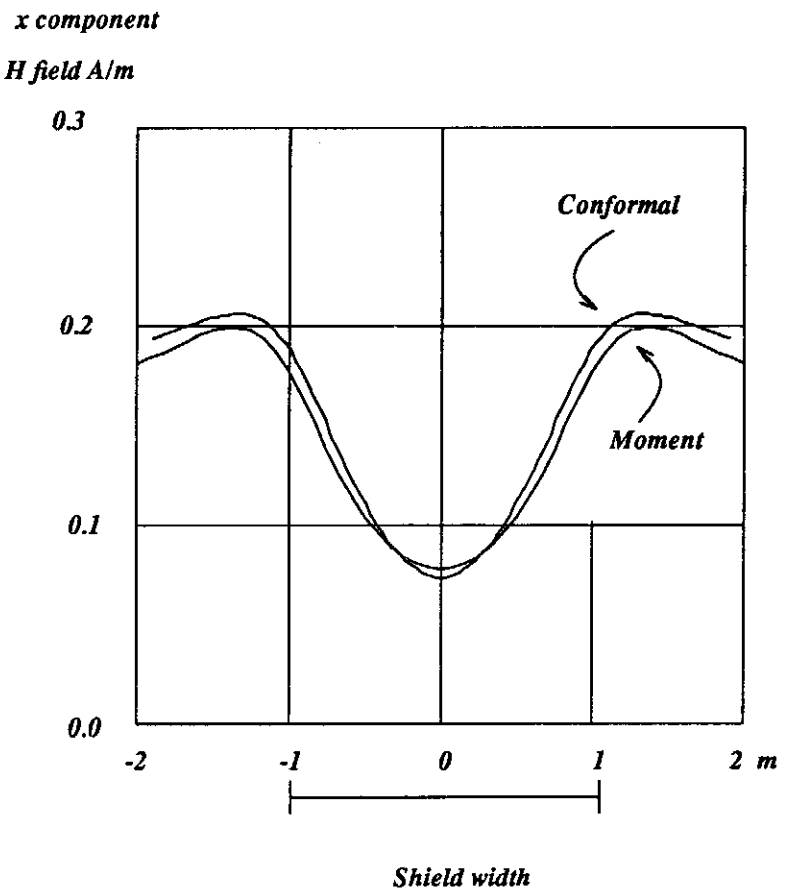

Figure 7. Comparison of single term moment method with conformal mapping solution.

Even with only a single term the approximation is quite good. Figure 8 is a three dimensional plot of the variation of the x component of the magnetic field for a distance 0.5 to 2 meters above the shield. In this example we consider a single basis function, $N=1$, to illustrate the effectiveness of a well chosen function. Moreover, it most be pointed out that using more terms of the basis functions (Equation 11), e.g., $N=2$ and $N=3$, improves the accuracy of the solution much like it does in the high frequency analog.

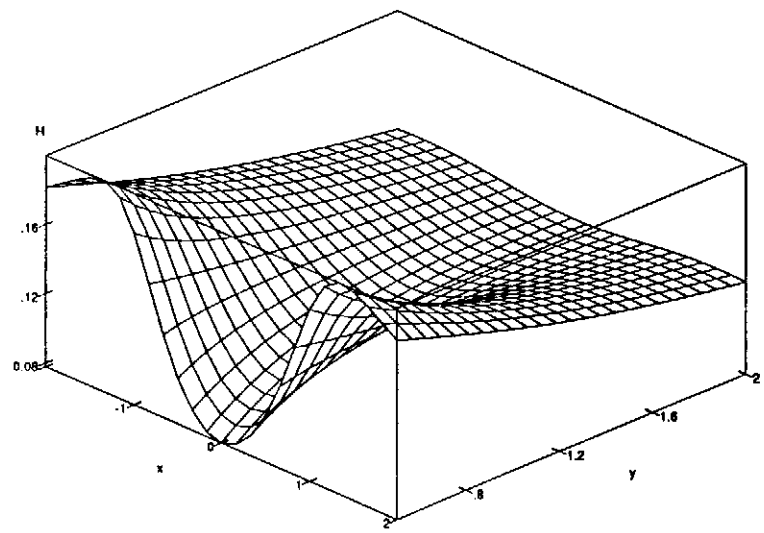

Figure 8. Magnetic field variation with position for a shield 2 meters wide with a source at -5 meters

Finally, consider the case of a thin strip of finite conductivity (or permeability). Using Parseval's theorem on the last term in equation (12),

$$\int_{-\infty}^{\infty} \tilde{\psi}_n(\alpha)\tilde{E}^{total}(\alpha)d\alpha = \int_{-1}^{1} \psi_n(-x)E^{total}(x)dx \ , \tag{13}$$

allows the replacement of the total electric field in the space domain by

$$\frac{\sum_{m=1}^{N} a_m J_m(x)}{\sigma + j\omega\varepsilon t} \tag{14}$$

for metal surfaces or

$$\frac{\sum_{m=1}^{N} a_m J_m(x)}{j\omega\mu t} \tag{15}$$

for high permeability surfaces, where σ, ε, μ, and t are the surface conductivity, the permittivity, the permeability, and the sheet thickness. In the next figure the strip example is again considered with finite permeability. The graphs show that as the permeability thickness product decreases the degree of shielding decreases.

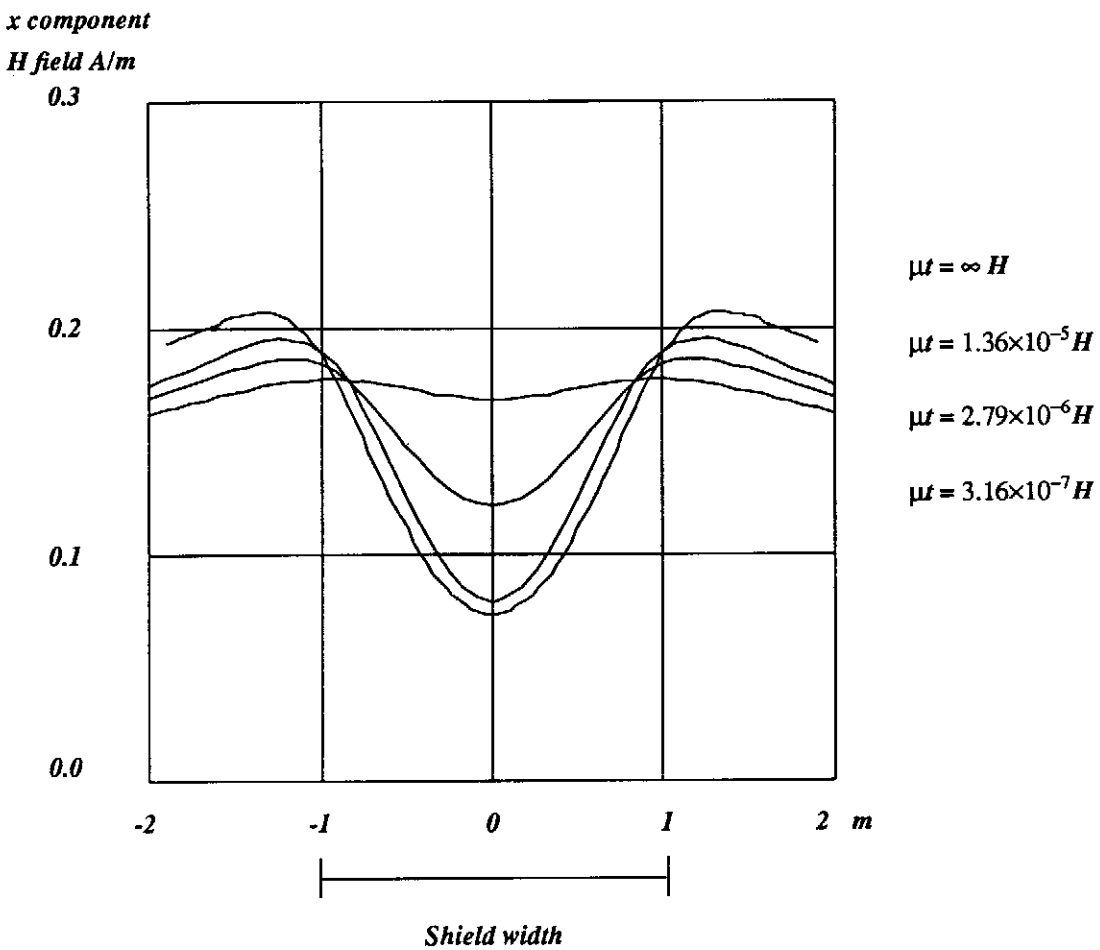

Figure 9. Field lines for source at -5 m. and shield 2 m. wide centered at the origin with $\mu t = \infty$, 1.36×10^{-5}, 2.79×10^{-6}, 3.16×10^{-7} H

3. Conclusions

It is shown that the moment method and the spectral domain techniques developed for high frequency applications may be successfully adapted for low frequency applications. The low frequency solutions found with the point collocation method and the spectral domain technique agree very well with the conformal mapping analytic solution and that unlike the static case, the finite permeability may be accounted for with relative ease. These are viable techniques for exploring cost effective high permeability inhomogeneous thin shields. The techniques may easily be extended to 3 dimensions for the analysis and design of thin inhomogeneous high permeability shields.

4. Appendix

Given the definition of the magnetic vector potential

$$\mathbf{A}=\frac{\mu}{4\pi}\int_{-\infty}^{\infty}\int\int \mathbf{J}(x',y',z')\frac{e^{\left[-j\beta\sqrt{\rho^2+(z-z')^2}\right]}}{\sqrt{\rho^2+(z-z')^2}}dx'dy'dz' \tag{A1}$$

and the current density

$$\mathbf{J}(x,y,z)=J_{ex}(x)\delta(y) \tag{A2}$$

where $\rho=\sqrt{(x-x')^2+(y-y')^2}$ and $\delta()$ is the Dirac delta function, the vector potential becomes

$$A_x=\frac{\mu}{4\pi}\int_{-\infty}^{\infty}\int_{-\infty}^{\infty}J_{ex}(x')\frac{e^{\left[-j\beta\sqrt{\rho^2+z'^2}\right]}}{\sqrt{\rho^2+z'^2}}dx'dz' \ , \tag{A3}$$

where $\rho=\sqrt{(x-x')^2+y^2}$ has been re-defined and z is assumed to be finite. Equation A3 may be recast as follows

$$A_x=\frac{j\mu}{4}\int_{-\infty}^{\infty}\frac{-j}{\pi}\int_{-\infty}^{\infty}J_{ex}(x')\frac{e^{\left[-j\beta\sqrt{\rho^2+z'^2}\right]}}{\sqrt{\rho^2+z'^2}}dx'dz' \ . \tag{A4}$$

The following substitutions

$$\beta\sqrt{\rho^2+z'^2}=\beta\rho\cosh t \tag{A5}$$

$$\frac{-jdz'}{\sqrt{\rho^2+z'^2}}=dt \tag{A6}$$

transforms Equation A4 into

$$A_x=\frac{j\mu}{4}\int_{-\infty}^{\infty}\frac{-j}{\pi}\int_{-\infty}^{\infty}J_{ex}(x')e^{\left[-j\beta\rho\cosh t\right]}dx'dt \tag{A7}$$

Equation A7 in conjunction with the integral definitions of the Bessel functions of the first and second kind, yields the desired vector potential.

$$A_x=\frac{j\mu}{4}\int_{-\infty}^{\infty}J_{ex}(x')H_0^{(2)}(\beta\rho)dx' \ . \tag{A8}$$

The x component of the electric field may be found from the vector potential as follows:

$$\begin{aligned}E_x^{scat}&=\frac{-j}{\omega\mu\varepsilon}\left[\frac{\partial^2}{\partial x^2}+\beta^2\right]A_x \\ &=\frac{-\eta}{4\beta}\int_{-\infty}^{\infty}J_{ex}(x')\left[\frac{\partial^2}{\partial x^2}+\beta^2\right]H_0^{(2)}(\beta\rho)dx' \ ,\end{aligned} \tag{A9}$$

where ω is temperal angular frequency. Evaluation of A9 and Bessel function identities yields

$$E_x^{scat} = \frac{-\eta}{8\beta} \int_{-\infty}^{\infty} J_{ex}(x')[H_0^{(2)}(\beta\rho)+H_2^{(2)}(\beta\rho)]dx' \tag{10}$$

where η is the free space impedance.

5. Acknowledgments

The authors wish to thank Harrison Rowe, Tim Hart, and Frank Boesch for their stimulating conversations.

REFERENCES

1. Harrington, R., *Field Computation by Moment Methods* (Reprint Edition), R.E. Krieger, Malabar, Fla., 1987; Original Edition, 1968.

2. Hechtman, C. and Levine, Z., *An Electrostatic Solution to a Specialized Routing Problem,* J. Appl. Phys., 62(5), pp. 2116-2122, 1 Sept. 1987.

3. Booton, R.C., *Computational Methods for Electromagnetics and Microwaves*, Wiley, 1992.

4. C. Balanis, *Advanced Engineering Electromagnetics*, pp. 707-717, J. Wiley, New York, 1989.

5. C. Scott, *The spectral domain method in electromagnetics*, Artech House, Norwood, Ma, 1989.

6. C. Balanis, *Advanced Engineering Electromagnetics*, pp. 310-312.

7. C. Balanis, *Advanced Engineering Electromagnetics*, pp. 702-705.

8. C. Balanis, *Advanced Engineering Electromagnetics*, pp. 681-683.